Periodically poled ridge waveguides in KTP for second harmonic generation in the UV regime

CHRISTOF EIGNER,[1,*] MATTEO SANTANDREA,[1] LAURA PADBERG,[1] MARTIN F. VOLK,[2] CHRISTIAN E. RÜTER,[2] HARALD HERRMANN,[1] DETLEF KIP,[2] AND CHRISTINE SILBERHORN[1]

[1]Department of Physics, University of Paderborn, 33098 Paderborn, Germany
[2]Faculty of Electrical Engineering, Helmut Schmidt University, 22043 Hamburg, Germany
*christof.eigner@uni-paderborn.de

Abstract: Waveguide circuits play a key role in modern integrated optics and provide an appealing approach to scalability in quantum optics. We report on periodically poled ridge waveguides in z-cut potassium titanyl phosphate ($KTiOPO_4$ or KTP), a material that has recently received growing interest due to its unique dispersion properties. Ridges were defined in surface-near rubidium-exchanged KTP by use of a precise diamond-blade dicing saw. We fabricated single-mode ridge waveguides at around 800 nm which exhibit widths of 1.9-3.2 μm and facilitated type-II second harmonic generation from 792 nm to 396 nm with high efficiency of 6.6 %/W·cm^2. Temperature dependence of the second harmonic process was found to be 53 pm/K. The low temperature dependence and high nonlinear conversion efficiency make our waveguides ideally suited for future operations in classical nonlinear integrated optics and integrated quantum networking applications.

References and links

1. K. Kato "Temperature Insensitive SHG at 0.5321 μm in KTP," IEEE J. Quant. Electron. **28**(10), 1974–1976 (2013).
2. J. D. Bierlein and H. Vanherzeele, "Potassium titanyl phosphate: properties and new applications," J. Opt. Soc. Am. B **6**(4), 622–633 (1989).
3. V. Ansari, E. Roccia, M. Santandrea, M. Doostdar, C. Eigner, L. Padberg, I. Gianani, M. Sbroscia, J. M. Donohue, L. Mancino, M. Barbieri, and C. Silberhorn, "Heralded generation of high-purity ultrashort single photons in programmable temporal shapes," Opt. Express **26**(3), 2764–2774 (2018).
4. G. Harder, V. Ansari, B. Brecht, T. Dirmeier, C. Marquardt, and C. Silberhorn, "An optimized photon pair source for quantum circuits," Opt. Express **21** (12), 13975–13985 (2013).
5. H. Karlsson and F. Laurell, "Electric field poling of flux grown $KTiOPO_4$," Appl. Phys. Lett. **71**(24), 3474–3476 (1997).
6. H. Karlsson, F. Laurell, and L. K. Cheng "Periodic poling of $RbTiOPO_4$ for quasi-phase matched blue light generation," Appl. Phys. Lett. **74**(11), 1519–1521 (1999).
7. J. Hellström, R. Clemens, V. Pasiskevicius, H. Karlsson and F. Laurell, "Real-time and in situ monitoring of ferroelectric domains during periodic electric field poling of $KTiOPO_4$," J. Appl. Phys. **90**(3), 1489–1495 (2001).
8. K. Laiho, K. N. Cassemiro, and C. Silberhorn "Producing high fidelity single photons with optimal brightness via waveguided parametric down-conversion," Opt. Express **17**(25), 22823 (2009).
9. H. Rütz, K. H. Luo, H. Suche, and C. Silberhorn, "Quantum Frequency Conversion between Infrared and Ultraviolet," Phys. Rev. Appl. **7**(2), 024021 (2017).
10. M. Rüsing, C. Eigner, P. Mackwitz, G. Berth, C. Silberhorn, and A. Zrenner, "Identification of ferroelectric domain structure sensitive phonon modes in potassium titanyl phosphate: A fundamental study," J. Appl. Phys. **119**(4), 044103 (2016).
11. M. F. Volk, C. E. Rüter, and D. Kip, "Rb/Ba side-diffused ridge waveguides in KTP," Opt. Express **25**(17), 19872–19877 (2017).
12. M. F. Volk, C. E. Rüter, M. Santandrea, C. Eigner, L. Padberg, H. Herrmann, C. Silberhorn, and D. Kip, "Fabrication of low-loss Rb-exchanged ridge waveguides in z-cut $KTiOPO_4$," Opt. Mater. Express **8**(1), 82–87 (2018).
13. L. G. Carpenter, S. A. Berry, and C.B.E. Gawith, "Ductile dicing of $LiNbO_3$ ridge waveguide facets to achieve 0.29 nm surface roughness in single process step" Electron. Lett. **53**(25), 1672–1674 (2017).
14. P. T. Callahan, K. Safak, P. Battle, T. D. Roberts, and F. X. Kärtner, "Fiber-coupled balanced optical cross-correlator using PPKTP waveguides," Opt. Express **22**(8), 9749–9758 (2014).

15. S. Müller, T. Calmano, P. W. Metz, C. Kränkel, C. Canalias, C. Liljestrand, F. Laurell, and G. Huber, "Highly efficient continuous wave blue second-harmonic generation in fs-laser written periodically poled Rb:KTiOPO$_4$ waveguides," Opt. Lett. **39**(5), 1274–1277 (2014).
16. R. Machulka, J. Svozilík, J. Soubusta, J. Peřina, and O. Haderka, "Spatial and spectral properties of fields generated by pulsed second-harmonic generation in a periodically poled potassium-titanyl-phosphate waveguide," Phys. Rev. A **87**(1), 013836 (2013).
17. A. Zukauskas, V. Pasiskevicius, and C. Canalias, "Second-harmonic generation in periodically poled bulk Rb-doped KTiOPO$_4$ below 400 nm at high peak-intensities," Opt. Express **21**(2), 1395–1403 (2013).
18. F. Laurell, J. B. Brown, and J. D. Bierlein, "Sum-frequency generation in segmented KTP waveguides," Appl. Phys. Lett **60**(9), 1064 (1992).
19. I. Shoji, T. Kondo, A. Kitamoto, M. Shirane, and R. Ito, "Absolute scale of second-order nonlinear-optical coefficients," J. Opt. Soc. Am. B **14**(9), 2268–2294 (1997).
20. A. Arie, G. Rosenman, V. Mahal, A. Skliar, M. Oron, M. Katz, and D. Eger, "Green and ultraviolet quasi-phase-matched second harmonic generation in bulk periodically-poled KTiOPO$_4$," Opt. Commun. **142**(4), 265–268 (1997).

1. Introduction

Potassium titanyl phosphate (KTiOPO$_4$ or KTP) is a well known and established material in bulk optics. A typical application for bulk KTP crystals is frequency doubling, for example in Nd:YAG lasers from 1064 nm to 532 nm [1]. KTP offers the advantage of a wide transparency range (365-4300 nm), which, in combination with the large nonlinear coefficients of the material, allows for applications with high power densities and therefore high efficiencies in the visible wavelength range. The high mechanical and chemical resistance and the low refractive index change with temperature make KTP devices stable against temperature fluctuations and changes in humidity [2]. Furthermore, unique dispersion properties make KTP the material of choice for a variety of quantum optical systems [3]. In particular, KTP is the only material that provides the dispersion required to build high brightness sources of high quality pure photons at telecom wavelengths without external filtering [4]. Another key property of KTP is its higher resistance against photorefraction at room temperature as compared to lithium niobate (LN). This enables high pump powers without the need for thermal stabilization at high temperatures, resulting in excellent performance even, at room temperature. The coercive field strength of KTP, that is the electric field strength required to invert the spontaneous polarization of the crystal, is one order of magnitude lower than for congruent LN ($E_c^{(KTP)} = 2.1$ kV/mm, $E_c^{(LN)} = 21$ kV/mm [5]). This means that periodic poling (PP), a prerequisite for many nonlinear optical processes to date, can be achieved in KTP with significantly less technical effort than in LN. These properties also make KTP an attractive candidate for integrated optics [8].

To exploit the benefits of tightly confined fields in integrated nonlinear optical devices, reliable fabrication techniques for waveguide structures are required. Several attempts have been made to fabricate waveguides in KTP, but the outstanding challenge remains in the development of a repeatable fabrication process of homogeneous waveguides which is compatible with periodic poling of the material. In this work, we exploit a diamond-blade dicing technique to fabricate ridge waveguides in periodically poled KTP.

Periodically poled rubidium-exchanged waveguides are attractive for down-conversion using type-II phase-matching, in which the photons are produced with definite orthogonal polarizations, as they guide light in both TE and TM polarization with low propagation losses. Further, these waveguides can be used to generate light in the UV regime or aim for frequency conversion interfacing short wavelength quantum memories, e.g. Yb$^+$, with telecom wavelengths [9]. We fabricated waveguides using a planar surface-near Rb-exchange (Rb:PPKTP) to achieve confinement in the depth direction. The lateral confinement is realized by a subsequent dicing process producing ridge waveguides. This offers an increased performance of the device due to a higher mode confinement and therefore higher mode overlap. The unique portfolio of properties, such as low photorefraction, mechanical and chemical stability, low coercive field strength and many more makes periodically poled Rb:KTP ridge waveguides highly desirable for integrated

(quantum) optical applications [11]. Here, we present fabrication of the first periodically poled KTP ridge waveguides. We analyse the performance of these ridge waveguides and demonstrate efficient second harmonic generation (SHG) with an efficiency of 6.6 %/W·cm^2.

2.   Sample fabrication

We fabricated ridge waveguides in KTP samples with dimensions of $14 \times 6 \times 1 \, mm^3$ along the crystallographic a, b and c axes, cut from a commercially available flux-grown wafer. An overview of the process is given in Fig. 1(a). First, the samples were immersed in a pure KNO_3 melt at 375 °C for 24 h, which homogenizes the sample composition and improves the diffusion and poling homogeneity. This KNO_3 treatment is necessary in samples which exhibit a large ionic conductivity. (Nowadays, due to the improved quality of commercial wafers this KNO_3 treatment may be redundant.) In a second step, the samples were periodically poled with periods from 7.2 μm to 7.5 μm. On the -c facet a periodic resist structure was defined in a lithographic process. Both sides (+c and -c) were coated with a metallic layer to provide electrical contact. We applied five high voltage pulses of 2.3 kV to invert the spontaneous polarisation. The pulses had a trapezoidal shape with 1 ms rising and falling time and a 2 ms plateau. To control the poling progress, we used an in-situ monitoring technique (as developed by Karlsson et al. [6, 7]) which is based on electro-optically induced polarisation rotation of a laser beam. After successful poling, we removed the metal electrodes and photoresist in an ammonia solution. This solution simultaneously acts as a selective etchant and all samples were etched to a depth of about 5 nm to visualize the domain structure, see Fig. 1(b). By increasing the etching time and temperature, topographic patterns up to 100 nm can potentially be achieved. A drawback of this method is the increased roughness of the surface which also increases the waveguide losses. A better, non destructive method to visualize the domain structure is confocal Raman spectroscopy [10]. Next, we fabricated waveguides in the periodically poled substrates. For the mode confinement in the depth direction, a planar waveguides was formed by ion exchange in a Rb nitrate ($RbNO_3$) bath at 330 °C for 1 h. The exchange depth of 6.2 μm was determined (with an accuracy of up to ±0.4 μm) by energy-dispersive X-ray spectroscopy (EDX) measurements of the Rb concentration with an electron beam microscope. The exchange depth d is defined assuming the rubidium concentration profile $c_{Rb}(z) = c_{Rb,0} \cdot [1 - \mathrm{erf}(z/d)]$ [12], where $c_{Rb,0}$ is the concentration at the surface.

Subsequent ridge definition was performed with a diamond-blade dicing saw, as shown in Fig. 1(a). The detailed fabrication steps of the dicing process are described in [12]. These ridges were diced into the former -c facet parallel to the a-axis. After preparing the ridges, the end facets were also prepared for light coupling by dicing. Scanning electron microscope (SEM) images of completed ridge waveguides are presented in Fig. 1(b and c), showing sharp edges and smooth surfaces. Using a white light interferometer, we measured a side wall roughness of 1-2 nm. In comparison, in lithium niobate surface roughness of 0.29 nm could be achieved in a single dicing step [13]. We prepared ridges of widths between 1.9 μm and 12 μm and heights between 10 μm and 20 μm. Due to the Rb-exchange, the waveguides are brittle and can be easily damaged by mechanical stress, e.g. during the dicing process. The dicing technique is not ideal for end facet preparation because chipping reduces the end facet quality. Therefore, quantitative loss measurements and mode field analysis measurements were only possible on a few waveguides of the present sample. An improved end facet preparation technique is currently under development.

3.   Waveguide properties

For the SHG experiments we used ridge waveguides with 2.6 μm to 3.6 μm width and a height of 17 μm, which is significantly higher than the Rb diffusion. First, we studied their linear optical properties. We found that narrow ridges guided a single mode at the fundamental wavelength of 800 nm. At a ridge width of 3.2 μm, a second mode appeared. We measured the near field of the
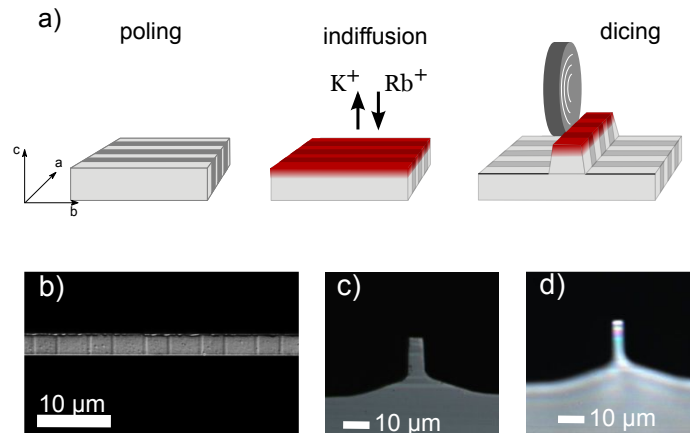
Fig. 1. a) Waveguides were formed in periodically poled KTP by Rb in-diffusion and subsequent ridge definition. SEM image of b) a selectively etched surface of a periodically poled ridge (top view) and of a c) waveguide's end facet; d) light image of a waveguide's end facet.

fundamental modes at 800 nm (see Fig. 2(b)). By knowing the waveguide width and exchange depth, we used a finite element method program (FEMSim tool from RSoft) to reproduce the measured mode. The fitting parameter was the refractive index increase at the surface. For the refractive index increase at the surface we thereby estimated Δn_{TE} = 0.011 ± 0.005 for TE and Δn_{TM} = 0.011 ± 0.005 for TM polarisation. The field overlap of the calculated and the measured mode was above 0.96, for both TE and TM modes, indicating a good fit. In Fig. 2(b) the calculated modes are indicated by white dashed lines. Total transmission through the waveguide was measured at a wavelength of 794 nm. For TE polarisation we measured a total transmission of 29.6 % and for TM 25.3 %. These values were corrected for Fresnel reflections, but not for the coupling efficiency. Assuming a perfect coupling efficiency, we can determine from the transmission measurement an upper limit for the waveguide losses of 6 dB/cm. However, we know that the quality of the end facet, and thus the coupling efficiency, has been the limiting factor of these measurements. Hence, we assume that the real waveguide losses are much lower, which could also be confirmed by characterising comparable samples, which have losses of about 1.5 dB/cm in the telecom range [12].

4. Second harmonic generation

We used waveguides with poling periods in the range from 7.35 μm to 7.50 μm to characterize the nonlinear behaviour using a second harmonic analysis. Linearly polarized light at 45° with respect to the c-axis from a continuous-wave Ti-sapphire laser (M2 SolsTis, M^2<1.1, linewidth ≤10 MHz) was coupled into the ridge waveguide with an 8 mm focal length lens (NA=0.5). Power and polarization were controlled with a polarizing beam splitter and a half-wave plate. In the waveguide, horizontally polarized light was generated in a type-II phase-matched process at half of the pump wavelength. After the waveguide, we used a short-pass and a colour glass filter to suppress the pump light. The generated light was detected with a power meter as a function of the fundamental wavelength. The measured phase-matching curve is shown in Fig. 3(a), blue line. Measurements essentially showed the expected $sinc^2$ function, with superimposed Fabry-Perot type oscillations. We attribute deviations from the envelope $sinc^2$ function to inhomogeneities in the poling and the waveguide itself. Fast oscillations arising from resonances within our setup
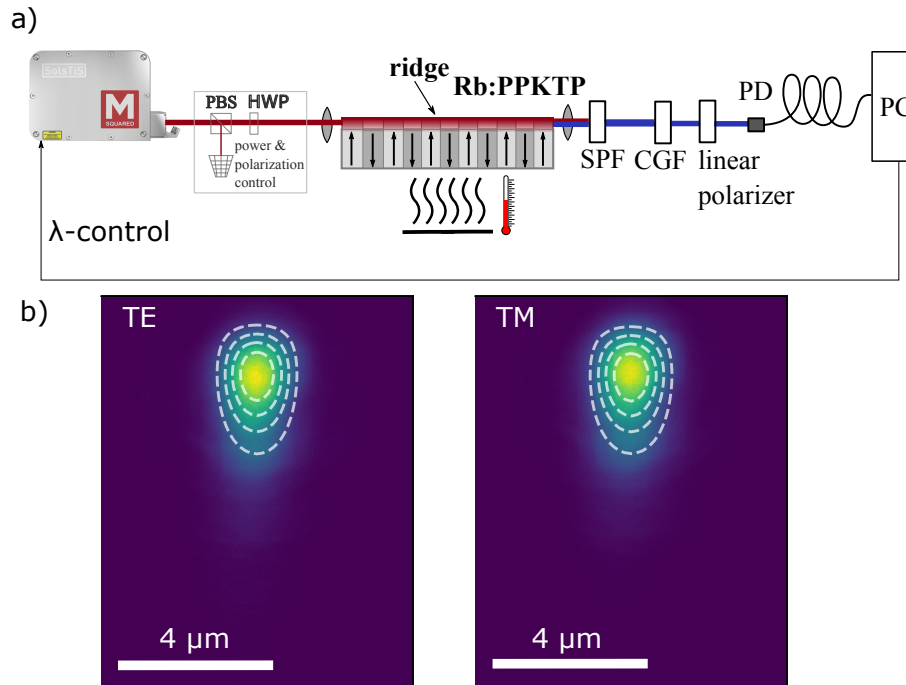
Fig. 2. a) Setup to investigate second harmonic generation in KTP ridge waveguides. The light was detected on a power meter. b) Experimentally obtained mode images of a 3.1 μm wide ridge waveguide at 800 nm, the calculated modes are indicated by white dashed lines, according to 20%, 40%, 60% and 80% of the simulated field amplitude.

are smoothed out during the integration time of the measurement. We attribute these resonances to interference occurring between optical components in our setup.

We fitted a sinc^2 function

$$P_{\text{SHG, norm}} = \text{sinc}^2\left(\Delta k \frac{l}{2}\right), \tag{1}$$

to the measured data. Here Δk represents the phase mismatch

$$\Delta k = \frac{2\pi \cdot n_{\text{y-eff}}(\lambda_{\text{SH}})}{\lambda_{\text{SH}}} - \frac{2\pi \cdot n_{\text{y-eff}}(\lambda_{\text{pump}})}{\lambda_{\text{pump}}} - \frac{2\pi \cdot n_{\text{z-eff}}(\lambda_{\text{pump}})}{\lambda_{\text{pump}}} - \frac{2\pi}{\Lambda}. \tag{2}$$

For the indices $n_i(\lambda)$ we used the Sellmeier equations for bulk KTP $n_{i(\text{bulk})}(\lambda)$ [1] and a modification to describe the refractive index increase of the rubidium in-diffusion $\Delta n_{i(\text{waveguide})}(\lambda)$ [14]

$$n_i(\lambda) = n_{i(\text{bulk})}(\lambda) + \Delta n_{i(\text{waveguide})}(\lambda). \tag{3}$$

It has to be noted that we are using, for the bandwidth calculation, the refractive index increase at the surface of the waveguide. The maximum of the sinc^2 function was set to the maximum of the data, and the fitting parameter was the effective length l_{eff}, which is reduced compared to the length of the periodically poled area. Longer poling lengths lead to smaller phase-matching bandwidths. Any error in the poling (e.g. missing domains) or the waveguide symmetry broadens the phase-matching bandwidth. We obtained the best fit for an effective length of 2.75 mm (Fig. 3(a), red line). The discrepancy to the theoretical curve for the actual poling length of $l = 7.9$ mm (Fig. 3(a), green dashed line) can be explained by inhomogeneous poling and variation of the
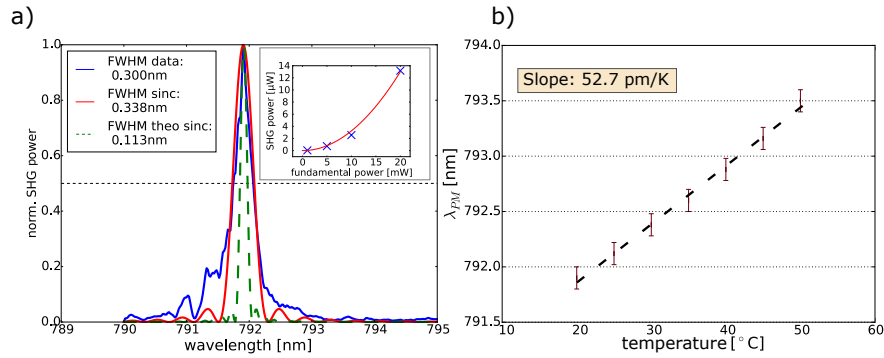
a)

b)

Fig. 3. a) Measured (blue) and calculated (red) phase-matching curve of a 2.6 μm wide and 7.9 mm long ridge waveguide for type-II conversion; the calculated curve (green) corresponds to a poling length equal to the sample length of 7.9 mm. The inset shows the Input-Output curve of fundamental to second harmonic power. b) Temperature dependence of the phase-matching wavelength.

diffusion profile and ridge width along the waveguide. The SHG efficiency was calculated as

$$\eta_{\text{exp}} = \frac{P_{\text{SHG}}}{P_{\text{pump}}^2 \cdot l^2} \cdot 100\% = 6.6 \, \frac{\%}{\text{W} \cdot \text{cm}^2}, \tag{4}$$

where P_{SHG} is the second harmonic (SH) power, P_{pump} is the pump power behind the waveguide and l is the length of the poled fraction of the crystal. The efficiency was corrected for end facet reflection losses, transmission losses of the short-pass filter (transmission T=0.85) and transmission losses of the coloured glass filter (T=0.86). The highest conversion efficiency of $\eta_{\text{exp}} = 6.6 \, \%/\text{W} \cdot \text{cm}^2$ was found for a 2.6 μm wide ridge of length $l = 7.9$ mm, a poling period of 7.35 μm, a pump wavelength of 792.2 nm and a pump power of 11.3 mW, resulting in a second harmonic power of 4.9 μW. A comparison of normalized efficiency with previous demonstrations of SHG in PPKTP waveguides is shown in Table 1.

Table 1. Comparison of efficiency for periodically poled bulk or waveguides in KTP.

	material	type	pump	second harmonic wavelength [nm]	efficiency
1	this work	II	cw	396.1	6.6 %/W·cm²
2	laser written waveguides in PPKTP [15]	II	cw	471	4.6 %/W·cm²
3	PPKTP wg [16]	II	pulsed	398.3	4.78 %/W·cm²
4	bulk KTP [17]	II	pulsed	398	1.79 %/W·cm
5	segmented KTP waveguides [18]	I	cw	425	122 %/W·cm²

We also determined the theoretically expected efficiency assuming no attenuation, perfect poling pattern and no index variation along the waveguide. Therefore, we calculated the overlap integral S by integrating the scalar amplitude of the electric field distributions of the two pump fields ($E_{\text{pump-TE}}$, $E_{\text{pump-TM}}$) and the SH field ($E_{\text{SH-TE}}$). We obtained these values from calculated modes in RSoft using the same refractive index increase for fundamental and second harmonic

mode. The obtained value of $S = 0.34\,\mu m^{-1}$ was used to calculate an expected efficiency of

$$\eta_{theo} = \frac{8\pi^2 d_{QPM}^2 S^2}{n^3 c \epsilon_0 \lambda_{pump}^2} = 12.4\ \frac{\%}{W \cdot cm^2}. \tag{5}$$

Here c is the speed of light, $n = 1.84$ is the refractive index of the SH wave [1], λ_{pump} is the pump wavelength, and $d_{QPM} = 2/\pi \cdot d_{24} = 2/\pi \cdot 1.9\,pm/V$ [19]. The deviation by a factor of 2 between experimental and theoretical efficiency is expected to be caused partially by waveguide losses, which arise especially for the higher order SH modes, and eventually by inaccuracy of the mode overlap calculation.

We measured the temperature dependence of the phase-matching to be 53 pm/K in a range from 20 °C to 60 °C (Fig. 3(b)), which is in good agreement with temperature dependent phase-matching measurements in PPKTP bulk crystals (60 pm/K) [20]. This result highlights the temperature insensitive behaviour which allows for stable operation, independently of the atmospheric conditions.

5. Conclusion

Using a diamond-blade dicing saw and Rb exchange, we have fabricated periodically poled ridge waveguides in z-cut KTP with low surface roughness which allows for relatively low losses. Furthermore, we successfully demonstrated type-II second harmonic generation (SHG) in a periodically poled (7.35 µm poling period) ridge waveguide. We analysed the performance of the ridge waveguides and demonstrated efficient second harmonic generation from 792.2 nm to 396.1 nm with normalized conversion efficiency of 6.6 %/W·cm². The measured bandwidth of 0.34 nm and the low temperature dependence of 53 pm/K pave the way for further exploration of a class of devices suitable for different and varying environments. Such z-cut ridge waveguides are good candidates for highly efficient nonlinear frequency conversion devices.